Journal of Plant Physiology 192 (2016) 47–55

Contents lists available at ScienceDirect

Journal of Plant Physiology

journal homepage: www.elsevier.com/locate/jplph

Biochemistry

Lotus japonicus plants of the Gifu B-129 ecotype subjected to alkaline stress improve their Fe^{2+} bio-availability through inoculation with *Pantoea eucalypti* M91

María Paula Campestre[a,1], Luis Nazareno Castagno[b,1], María Julia Estrella[b,2], Oscar Adolfo Ruiz[a,*]

[a] *Unidad de Biotecnología 1, Instituto de Investigaciones Biotecnológicas—Instituto Tecnológico de Chascomús/Consejo Nacional de Investigaciones Científicas y Técnicas—Universidad Nacional de San Martín (IIB—INTECH/CONICET—UNSAM), Avenida Intendente Marino Km 8,2 CC 164, B7130IWA Chascomús, Argentina*

[b] *Laboratorio de Microbiología del Suelo, Instituto de Investigaciones Biotecnológicas—Instituto Tecnológico de Chascomús/Consejo Nacional de Investigaciones Científicas y Técnicas—Universidad Nacional de San Martín (IIB-INTECH/CONICET-UNSAM), Avenida Intendente Marino Km 8,2 CC 164, B7130IWA Chascomús, Argentina*

ARTICLE INFO

Article history:
Received 9 October 2015
Received in revised form 5 January 2016
Accepted 5 January 2016
Available online 7 January 2016

Keywords:
Lotus japonicus
Alkaline soils
Fe deficiency
Pantoea sp.
PGPB

ABSTRACT

Inoculation assays with *Pantoea eucalypti* M91 were performed on *Lotus japonicus* ecotype Gifu. Under alkaline conditions, this ecotype is characterized by the development of interveinal chlorosis of the apical leaves due to low mobilization of Fe^{2+}. Inoculation with *P. eucalypti* M91, a plant growth-promoting bacterial strain capable of producing pyoverdine-like and pyochelin-like siderophores under alkaline growth conditions, alters the root, resulting in a herringbone pattern of root branching. Additional features include improvement in Fe^{2+} transport to the shoots, acidification of the hydroponic solution of the plant cultures, and an accompanying increase in the efficiency of the PSII parameters. In addition, there was an increase in the expression of the *FRO1* and *IRT1* genes, accompanied by a significant increase in FRO activity. Results showed that *P. eucalypti* M91 has a beneficial effect on the Fe acquisition machinery of Strategy I, as described for non-graminaceous monocots and dicots, suggesting its potential as an inoculant for legume crops cultivated in alkaline soils.

1. Introduction

Calcareous soils contain high concentrations of HCO_3^- and CO_3^{2-} that increase soil pH and limit Fe solubility. Plants require Fe for the proper functioning of multiple metabolic and enzymatic processes, such as those related to oxygen and electron transport, nitrogen fixation, DNA and chlorophyll biosynthesis, and photosynthesis (Eichert et al., 2010; Ivanov et al., 2012). Fe deficiency therefore induces certain conditions, particularly in young leaves, including interveinal chlorosis, which results from low concentrations of photosynthetic pigments, chlorophylls, and carotenoids (Abadia et al., 2000). As a result, photosynthetic rate, as well as light absorption, photosystem II (PSII), and RuBisCo efficiencies are markedly reduced (Larbi et al., 2006). These alterations have been reported previously in model and crop species of the *Lotus* genus (Babuin et al., 2014; Paz et al., 2012). Fe deficiency is a serious economic problem that severely affects crop quality and yields and requires expensive corrective methods to resolve. However, there is also an inexpensive, environmentally friendly biotechnological solution in which plants are inoculated with growth-promoting bacterial strains (Eichert et al., 2010).

Plants have developed several strategies to cope with Fe deficiency. In Strategy I, which occurs in non-graminaceous monocots and dicots, several physiological and morphological processes are used to increase Fe uptake (Ramírez et al., 2008; Romera et al., 2011; Ivanov et al., 2012; Wang et al., 2012). First, the surround-

Abbreviations: PSII, photosystem II; FRO, ferric reductase oxidase; IRT, iron regulated transporter; PGPB, plant growth promoting bacteria; CAS, chrome-azurol S; RFP, red fluorescent protein; DW, dry weight; PI, performance index; TT, topological tendency; RU, relative units; ANOVA, analysis of variance; VOC's, volatile organic compounds; IAA, indole-3-acetic acid.

* Corresponding author.
E-mail addresses: mpcampestre@intech.gov.ar (M.P. Campestre), ncastagno@intech.gov.ar (L.N. Castagno), estrella@intech.gov.ar (M.J. Estrella), ruiz@intech.gov.ar, oaruiz@conicet.gov.ar (O.A. Ruiz).

[1] These authors contributed equally to this work.

[2] This author is a member of the Research Career of Comisión de Investigaciones Científicas, Buenos Aires, Argentina (CIC).

http://dx.doi.org/10.1016/j.jplph.2016.01.001
0176-1617/

ing rhizosphere is acidified via proton extrusion by a root plasma membrane-localized proton ATPase in order to increase the solubility of Fe^{3+} complexes, after which Fe^{3+} is reduced to Fe^{2+} by ferric reductase oxidase 1 (FRO1). Subsequently, Fe^{2+} ions are taken up into root cells by the divalent iron regulated transporter 1 (IRT1) (Jain et al., 2014). Resulting morphological modifications include changes in root architecture, with enhanced development of lateral roots and differentiation of specialized transfer cells for increased surface area and improved performance (Guerinot and Yi, 1994). Meanwhile, Strategy II, or the chelation strategy, applies to graminaceous plants (Singh et al., 2013). In this case, extruded phytosiderophores chelate Fe^{3+}, after which the resulting complexes are imported by the surrounding roots (Guerinot and Yi, 1994; Romera et al., 2011; Ivanov et al., 2012). In nature, plants which are unable to adopt either of these strategies, or which have acquired them only partially, are classified as Fe-inefficient plants, and eventually develop interveinal chlorosis of the apical leaves in environments with low Fe content (Bacaicoa and García-Mina 2009; Von Wirén et al., 1993).

A wide variety of bacterial species broadly classified as Plant Growth Promoting Bacteria (PGPB) are capable of colonizing the rhizosphere and activating a mechanism similar to that of graminaceous plants growing in calcareous soils. Under the appropriate conditions, they synthesize and release siderophores, increasing and regulating Fe bio-availability. As a result, these PGPBs promote plant growth, improve the nutrition of the host plant, and protect it from biotic and abiotic stress factors (Zhang et al., 2009; Castagno et al., 2011; Zamioudis et al., 2013; Castagno et al., 2014; Jin et al., 2010). As a result, their role in plant nutrition has been studied in-depth (Crowley et al., 1988). Furthermore, many PGPBs exert other beneficial effects on plants, since they are able to solubilize phosphates and other micronutrients (Radzki et al., 2013). For example, *Pantoea eucalypti* M91 was isolated from alkaline soils and showed the ability to solubilize phosphates and Fe, serving as a PGPB for *Lotus tenuis* under both greenhouse (Castagno et al., 2011) and outdoor conditions (Castagno et al., 2014).

Lotus japonicus and *L. tenuis* are both legume species of the genus *Lotus*. *L. japonicus* is primarily of interest as a model plant for physiological and genetic studies, particularly those relating to the mechanisms involved in stress tolerance (Escaray et al., 2012; Bordenave et al., 2013; Babuin et al., 2014). In particular, *L. japonicus* is most commonly used in the laboratory as the Gifu B-129 (Gifu) or Miyakojima (MG-20) ecotype. Previous work has shown that they exhibit contrasting behavior under similar alkaline stress conditions, with MG-20 being tolerant and Gifu being sensitive (Babuin et al., 2014). To corroborate this observation, we adopted similar criteria, which have been valuable in evaluating other *Lotus* species under salt stress (Sanchez et al., 2011). Klein et al. (2012) also confirmed comparatively better performance of the MG-20 ecotype, in that case under low Fe concentrations. Considering these results, the principal aim of this research was to evaluate Fe^{2+} uptake by the Gifu ecotype in the presence of *P. eucalypti* M91, in the hopes of developing strategies for improved nutrition under alkaline stress.

2. Materials and methods

2.1. Bacterial strain, growth conditions, and siderophore production

P. eucalypti M91 (Castagno et al., 2011) was grown in TY media (Sperry and Wilkins, 1976). Siderophore production was determined in Chrome-azurol S (CAS) media as per the Universal Chemical Assay (Schwyn and Neilands, 1987). A bacterial suspension that was cultured for 24 h was spotted on a CAS plate and incubated at $28 \pm 1\,^{\circ}C$ for 48 h. The production of siderophores was indicated by the formation of an orange to yellow halo around the colonies. The siderophore types were assessed in the supernatant of samples that had been cultured for 72 h in minimal media (Carrillo and Peralta, 1988) containing either no Fe source or an $FeCl_3$ supplement (6 or 60 μM). The absorbance spectra were recorded using a Synergy H1 multi-mode reader, and revealed the presence of two maxima (355 and 405 nm) that correspond to pyochelin (Xiao and Kisaalita, 1995) and pyoverdine (Yang et al., 2011). The fluorescence emission spectra revealed maxima at 430 and 460 nm for excitation wavelengths of 355 and 405 nm, respectively, values that are consistent with pyochelin and pyoverdine (Yang et al., 2011; Dumas et al., 2013).

2.2. Plant material, plant growth conditions, and experimental design

Seeds of the *L. japonicus* Gifu ecotype were scarified with sulfuric acid (98%), washed in distilled water, and placed in Petri dishes containing water-agar (0.8%). The dishes were incubated in a growth chamber until cotyledons were observed using a 16/8 h photoperiod at 24/19 °C and 60/80 ± 5% relative humidity under fluorescent light bulbs providing 200 μmol photons $m^{-2}\,s^{-1}$. The same environmental conditions were used for all the treatments described below. During these treatments, plants were irrigated with half-strength Hoagland's nutrient solution (Hoagland and Arnon, 1950) composed of 3 mM KNO_3, 2 mM $Ca(NO_3)_2{\cdot}4H_2O$, 1 mM $MgSO_4{\cdot}7H_2O$, 0.5 mM $NH_4H_2PO_4$, 50 μM $NaFeO_8EDTA{\cdot}2H_2O$, 4.5 μM $MnCl_2{\cdot}4H_2O$, 23 μM H_3BO_3, 0.16 μM $CuSO_4{\cdot}5H_2O$, 0.09 μM $ZnSO_4{\cdot}7H_2O$, and 0.06 μM $Na_2MoO_4{\cdot}2H_2O$.

To determine total Fe content, gene expression, and root morphology, seedlings were transferred to their individual cylindrical pots (5.8 × 20 cm; v = 0.53 dm^3) containing sand that had been autoclaved twice. Experiments were completely randomized and tested, with four sets of treatments for control, alkalinity, control + inoculation, and alkalinity + inoculation. Alkalinity trials included 10 mM $NaHCO_3$ (pH 8.3). Inoculation with a *P. eucalypti* M91 bacterial suspension (1×10^8 cells per mL) was done during the transplant period. All seedlings were first irrigated for 1 week, followed by 3 week under the respective treatment. The irrigation system was as described by Paz et al. (2012).

For Fe^{2+} content, growth promotion, acidification of the hydroponic solution, and root FRO activity measurement, seedlings that had been cultivated in sand and irrigated with the nutrient solution for 15 days were removed and their roots rinsed with sterile deionized water, after which each seedling was transferred to a beaker containing 150 mL of sterile, half-strength Hoagland's nutrient solution. The nutrient solution was replaced every 3 days. The roots were protected from light by wrapping the beakers in black paper. All seedlings were grown for 1 week, followed by 2 week under the respective treatment. The bacterial suspension was added to the nutrient solution at the beginning of the solution culture and refreshed whenever the nutrient solution was replaced.

2.3. Evaluation of endophyte colonization capacity

In order to evaluate the endophytic bacteria on the roots and shoots of the plants, *P. eucalypti* M91 was designed to express the red fluorescent protein (RFP). The traceable strain was generated by four-parental mating conjugation, using the donor strain *Escherichia coli XL1-Blue* containing the plasmid *pBK-miniTn7*-Plac-rfp-GenR (Koch et al., 2001). In order to evaluate endophytic colonization, epifluorescence microscopy was used. During harvest, plants were divided into roots and shoots. Samples were analyzed with a Nikon Eclipse E600 microscope equipped with a

450–490 nm excitation filter and a 520 nm long pass emission filter. Images were acquired with a Nikon DS-Qi1Mc video camera.

2.4. Total Fe determination

To analyze Fe content, roots and shoots were collected separately, carefully washed with deionized water, and deposited in glass vials. Then, 100 mg of fresh material were reduced to ashes at 550 °C for 8 h. The samples were digested with 0.5 mL of 65% HNO_3 and diluted to a final volume of 3.5 mL with deionized water. Fe content was determined with an AAnalyst 100 atomic absorption spectrophotometer (PerkinElmer) in absorption mode. A 1000 mg Fe L^{-1} atomic spectroscopy standard was used (PerkinElmer).

2.5. Fe^{2+} content determination

Fe^{2+} content was determined according to Babuin et al. (2014). Shoots and roots were harvested, carefully washed with deionized water, frozen in liquid N_2, and stored at −80 °C until analysis. The organs were cut into small pieces with clean scissors. Tissue samples (100 mg) of each organ were stirred in 1.2 mL of 80 mM 2.2′-dipyridyl-HCl (pH 3.0) in 10% methanol in the dark (24 h). Extracts were passed through a 0.45 μm syringe filter, after which 1 mL of the filtrate was assayed at 522 nm using a spectrophotometer (Zeltec ZL-5000 UV/vis Spectrometer, Argentina). Fe^{2+} content was calculated from a standard curve using Fe atomic absorption standard solution (PerkinElmer).

2.6. Determination of the hydroponic solution pH and bacterial growth-promoting effect

The pH of the hydroponic solutions in the above treatments was measured immediately after nutrient solution was added, and again after 3 days using a digital pH meter. In addition, at harvest time, the plants which had been reserved for the determination of dry weight (DW) were oven-dried at 70 °C to constant weight.

2.7. Measurement of root ferric reductase activity

To measure ferric reductase activity, the root of each plant was rinsed with deionized water, after which the root tips were removed, weighed (Zouari et al., 2001), and transferred to a full-strength Hoagland's nutrient solution containing 0.1 mM Fe^{3+}-EDTA and 0.4 mM 2,2′-bipyridyl. After 1 h under the same growing conditions as those utilized for the seedlings, the solution was measured at 520 nm by a spectrophotometer (ZELTEC ZL-5000 UV/vis spectrometer; Argentina) for the formation of the Fe^{2+}-dipyridyl complex.

2.8. Measurement of fluorescence

Non-invasive chlorophyll fluorescence fast-transient test (JIP test) was performed 2 days before harvest according to Gazquez et al. (2015) on blades of the third expanded leaf with a portable chlorophyll fluorometer (Pocket PEA, Hansatech Instrument, UK). The JIP parameter maximum quantum yield of primary PSII photochemistry (F_V/F_M), the Performance Index (PI) and the Electron transport per reaction center (Et_o/Rc) were analyzed. For this purpose, leaves were covered with leaf clips to adapt them to darkness for 20 min. Then, leaf clips were opened, and samples were exposed during 3 s to 3500 μmol photons m^{-2} s^{-1} (637 nm peak wavelength). The pocket PEA software (PEA plus v1.1, Hansatech Instrument Ltd., UK) was used to analyze PSII properties according to Strasser et al. (2000).

2.9. Root topology

After the harvest, the roots were washed with water to remove any remaining sand and then carefully extended on a flat glass and scanned. The images were analyzed with Image-ProPlus v4.1 software (Media Cybernetics, Bethesda, MD, USA). Root topology was calculated as in Paz et al. (2012). Values of TT between 0 and 0.5 characterize the dichotomous pattern, while values between 0.5 and 1 characterize the herringbone pattern (Paz et al., 2012).

2.10. Gene expression

Total RNA was extracted from frozen shoots and roots using a Spectrum Plant Total RNA kit (Sigma) according to the manufacturer's instructions. RNA quality was checked by agarose gel electrophoresis. After this, a DNAase treatment with an Ambion TURBO DNA-free kit was performed. Samples were quantified using a Synergy H1 Multi-Mode Reader, allowing for the isolation of 2 μg of RNA for reverse transcription and cDNA synthesis.

Quantitative RT-PCR of Strategy I genes *FRO1* (ID: ljwgs_147904.1.1) and *IRT1* (ID: ljwgs_049882.1) was performed. In order to effect the analysis, 2.5 mL from a ten-fold dilution of the cDNA stock was further diluted to 15 mL with the primer mix (300 nM final concentration), 7.5 mL of Fast Start Universal SYBRH Green Master (Rox), and the required amount of double distilled water. The following primers were used: *FRO1* forward 5′-TGG TGA GTG GAG GAA GTG-3′, *FRO1* reverse 3′-TAG CAT TGA CAG AGA TGA AGA G-3′, *IRT1* forward 5′-TTC AAG ACC AAA GCA GTT AT-3′, *IRT1* reverse 5′-TCC ACA ATC AGA GCA GTT-3′. Reactions were

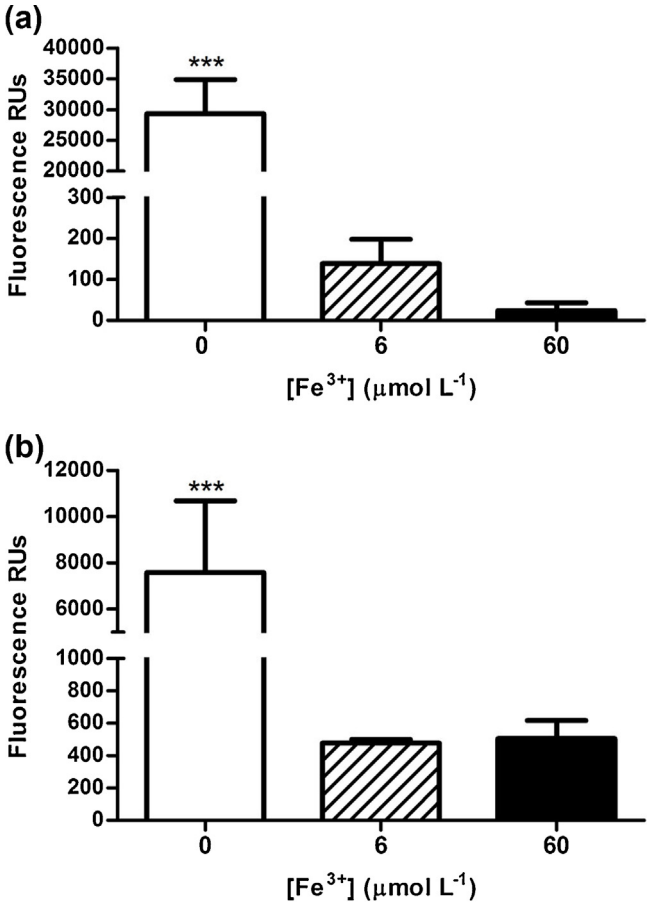

Fig. 1. Siderophore determination. (a) Pyoverdine-(λ_{exc} = 405 nm and λ_{em} = 460 nm) and (b) pyochelin-(λ_{exc} = 355 nm and λ_{em} = 430 nm) like siderophore levels determined for varying levels of $FeCl_3$ supplement. One-way ANOVA ($P < 0.001$).

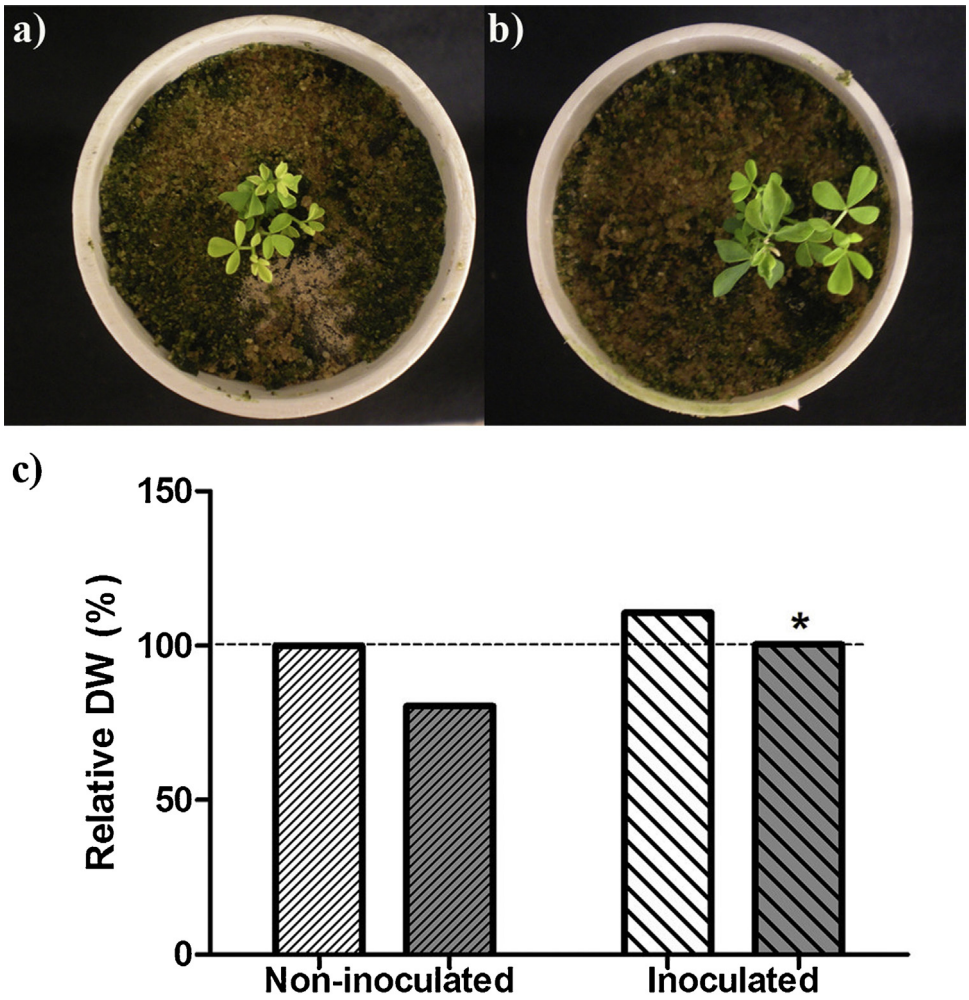

Fig. 2. Phenotype and growth response to inoculation. Phenotype photographs were taken after 21 days of alkaline treatment. (a) Alkalinization and (b) alkalinization and inoculation effects on shoots can be observed. (c) The growth promotion effect as a percentage of relative dry weight (DW) was determined for the entire plant. White bars represent control treatments and grey bars represent alkaline treatments (mean ± SD; $n = 5$). Asterisks represent significant differences between treatments. Student's *t*-test ($P < 0.05$).

performed in an Mx3005 P qPCR System with the help of the MxPro qPCR Software 4.0 (Stratagene, La Jolla, CA, USA). *EF* was used as the endogenous control (ID: AY633710). Results were expressed relative to the expression level of the control inoculated plants as relative units (RU), after being normalized to *EF* expression.

2.11. Statistical analysis

All statistical procedures were carried out using the INFOSTAT statistical package (Version 2010, group InfoStat, FCA, Universidad Nacional de Córdoba, Argentina). Significant differences were generally assessed using analysis of variance (ANOVA), while Student's *t*-test and Duncan's test were used to determine significant differences among the means.

3. Results

3.1. Characterization of the siderophores produced by P. eucalypti *M91*

A given microbial species may produce several siderophores (Marschner et al., 2011). The *P. eucalypti* M91 strain isolated and selected by our laboratory produced at least two types under Fe-limiting conditions, specifically pyoverdine-like (Fig. 1a) and pyochelin-like (Fig. 1b) siderophores. The relative fluorescence of the isolated culture supernatant showed that the production of both types increased significantly when the strain was cultivated without any Fe sources. Differences were also seen in pyoverdine-like siderophore levels upon comparing the 6 and 60 μM Fe supplementation (Fig. 1a).

Additionally, the *P. eucalypti* M91 strain harboring *RFP* expression was found as an endophytic in the roots and shoots of the model species, both in plants cultivated under control conditions and plants growing under alkaline stress (Fig. S1).

3.2. Evaluation of total Fe and Fe^{2+} content and growth promotion of the bacterial strain

The shoots from both inoculated and non-inoculated plants had higher total Fe content than those of the controls. Nevertheless, non-inoculated alkaline plants developed Fe chlorosis in the apical leaves (Fig. 2a). Therefore, Fe^{2+} content was considered a more appropriate measurement, as it represents the ionic form directly available to the metabolic processes.

Interestingly, the Fe^{2+} content in the shoots of plants cultivated under alkaline conditions was lower than in control plants (Table 1), which is consistent with the observed chlorosis. However, inoculation under alkaline conditions gave levels similar to those observed

Table 1
Total Fe and Fe^{2+} concentrations in the shoots and roots after 21 and 15 days, respectively, of alkaline treatment.

	Shoots		Root	
	Total Fe (mg/kg FW)	Fe^{2+} (mg/Kg FW)	Total Fe (mg/Kg FW)	Fe^{2+} (mg/kg FW)
G* control	17.383 ± 4.61b	12.108 ± 0.69a	168.062 ± 28.40a	3.528 ± 1.54c
G M91** control	21.680 ± 7.34b	12.190 ± 1.44a	156.838 ± 36.81 a	1.835 ± 1.03c
G* alkaline	39.666 ± 7.18a	6.902 ± 1.53b	77.315 ± 10.55b	15.599 ± 3.44a
G M91** alkaline	38.758 ± 8.81a	11.031 ± 0.67a	114.833 ± 27.68 a	9.095 ± 2.65b

Different letters indicate significant differences between treatments (as determined by the Duncan test and two-way ANOVA ($P < 0.05$)) ($n = 12$).
* G: non-inoculated.
** G M91: inoculated.

in control plants, leading to greening in young leaves (Fig. 2b). Furthermore, Fe^{2+} content was higher in the roots of inoculated plants cultivated under alkaline conditions than in those of the control plants, and even more so compared to non-inoculated plants cultivated under alkaline conditions (Table 1). In line with these results, there was a 20% reduction in DW of the non-inoculated plants exposed to alkaline stress when compared to the DW of the control plants (Fig. 2c). However, inoculated plants exposed to alkaline stress reached DW values similar to those of the non-inoculated control plants (Fig. 2c).

3.3. Measurement of PSII efficiency

Under control conditions, the mean F_V/F_M value was 0.825 for non-inoculated plants and 0.83 for inoculated plants (Fig. 3a). Under alkaline conditions, F_V/F_M fell in non-inoculated plants to 0.79, while it only fell to 0.81 in inoculated plants. As shown in Fig. 3b, the PI in non-inoculated plants decreased to approximately 25% of the control value when plants were subjected to alkaline stress, while that of the inoculated plants decreased less so, to 48%. The Eto/Rc index was also affected by alkalinity, with a decrease of approximately 50% in non-inoculated plants compared to control plants. However, inoculation increased electron transport by 25% (Fig. 3c).

3.4. Analysis of root morphology

Studies of root architecture use a topological model based on the arrangement of links in the root system (Paz et al., 2012). This model showed that control samples exhibited dichotomous root branching, with TT values near 0.2 (Fig. 4b and d). This root pattern did not change for non-inoculated samples subjected to alkaline stress, with values falling short of 0.5 (Fig. 4c). By contrast, inoculation yielded a more herringbone pattern, with TT values above 0.5 (Fig. 4e).

3.5. Evaluation of the pH of the culture medium

The baseline hydroponic solution pH was 6.50 for control plants and 8.30 for alkaline plants. Under control treatment, the pH of the hydroponic solutions of both inoculated and non-inoculated plants declined after 3 days (Fig. 5a). Meanwhile, under alkaline treatment, the pH of the solution of the non-inoculated plants did not significantly change (Fig. 5b). However, the pH for the inoculated plants declined from 8.30 to 7.66 after 3 days of alkaline treatment (Fig. 5b).

3.6. Determination of FRO activity

Fe availability by reduction of Fe^{3+} was estimated by determining FRO activity (Fig. 6). The plants exposed to alkaline conditions exhibited an increase in FRO activity with respect to the control plants. At the same time, higher FRO activity was measured in

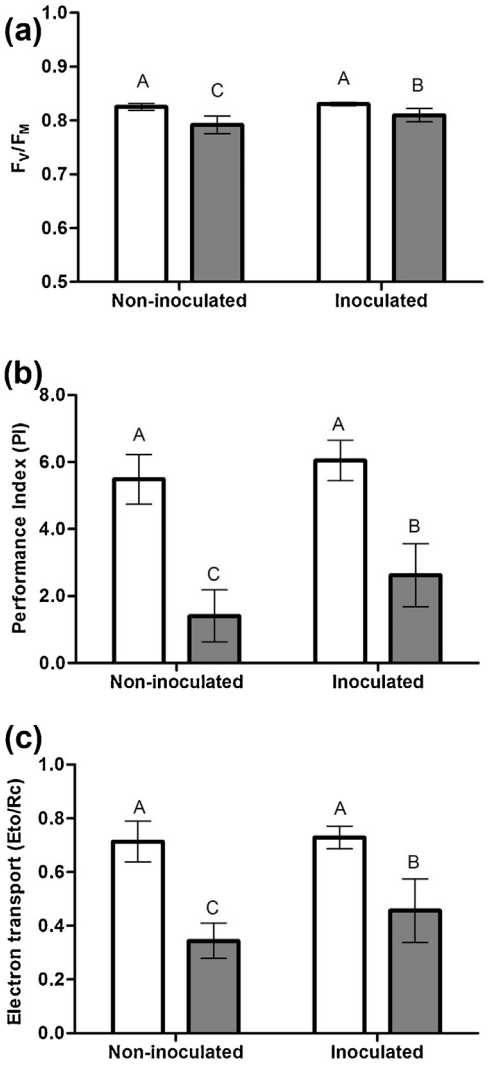

Fig. 3. PSII efficiency parameters. (a) F_v/F_m, (b) PI, and (c) Eto/Rc for samples subjected to alkaline treatment. White bars represent control treatments and grey bars represent alkaline treatments (mean ± SD; $n = 5$). Different letters indicate significant differences between treatments. Duncan test, two-way ANOVA ($P < 0.05$).

inoculated plants compared to the non-inoculated ones, resulting in even higher activity under alkaline stress and suggesting that the mere presence of the endophytic bacterial strain is enough to induce Fe^{3+} reduction.

3.7. Regulation of plant genes involved in the assimilation of soil Fe

The increase in FRO activity for alkaline conditions showed a corresponding increase in *FRO1* gene expression, with an expression

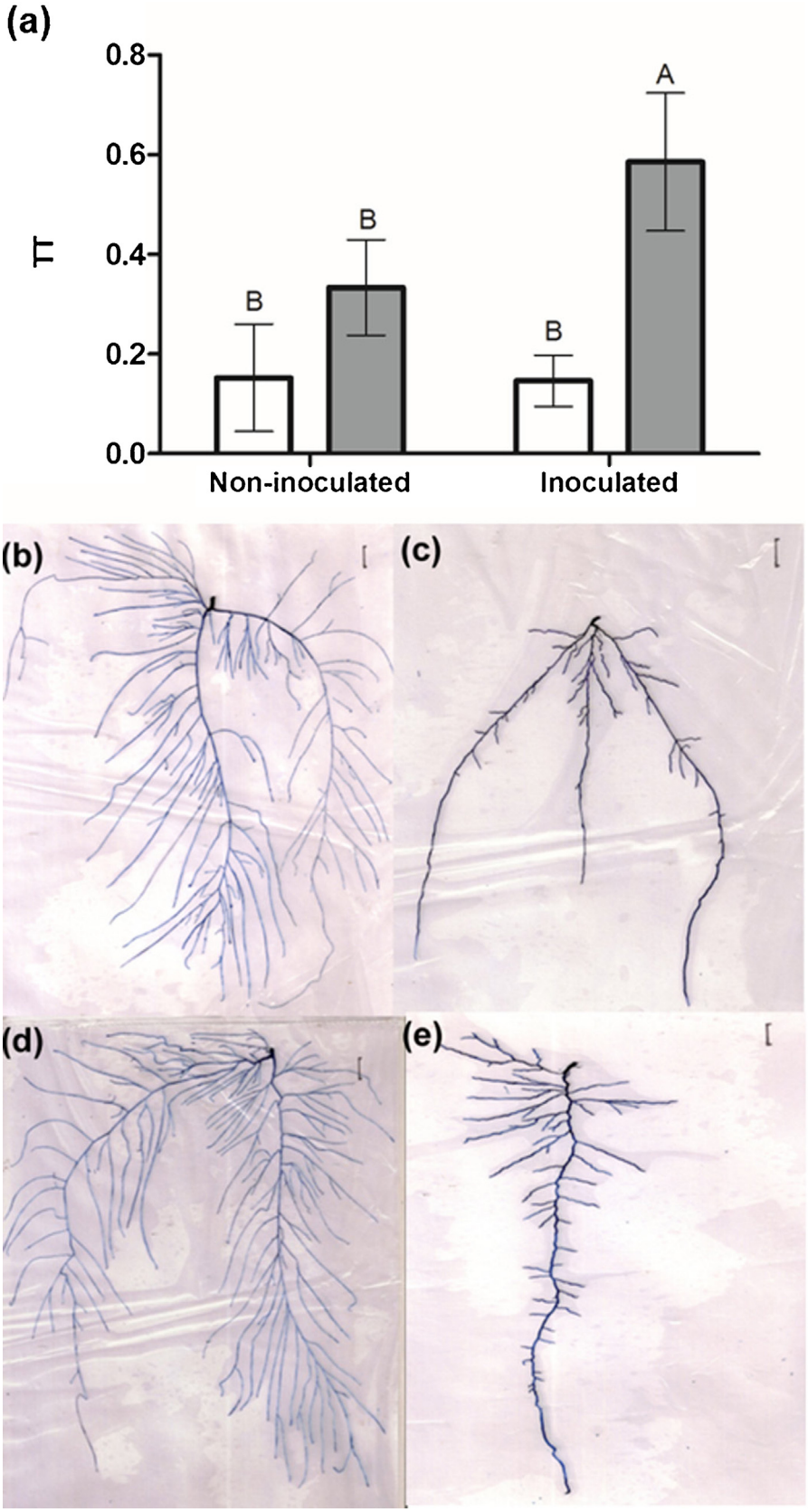

Fig. 4. Morphological root changes. (a) TT determination after 21 days of alkaline treatment. White bars represent control treatments and grey bars represent alkaline treatments (mean ± SD; $n = 12$). Different letters indicate significant differences between treatments. Duncan test, two-way ANOVA ($P < 0.05$).
A typical dichotomous pattern is seen in roots of (b) non-inoculated and (d) inoculated control plants and in (c) non-inoculated alkaline treated plants, while a typical herringbone pattern is seen in roots of (d) inoculated alkaline treated plants. Scale bars represents 1.0 cm.

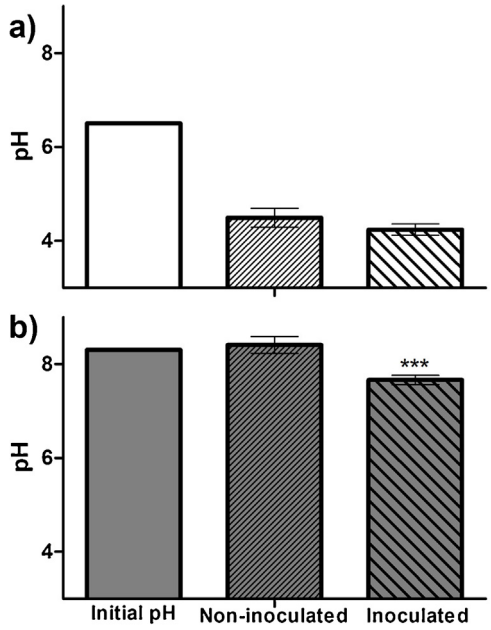

Fig. 5. Acidification of the hydroponic solution of culture plants. The extrusion of H^+ to the hydroponic solution by Gifu roots and by the inoculation with *P. eucalypti* M91 was determined by pH measurements at day 1 and 3 of alkaline treatment. (a) pH units at initial time (1 d) and for non-inoculated and inoculated control plants (3 d). (b) pH units at initial time (1 d) and for non-inoculated and inoculated alkaline plants (3 d). Bars (mean ± SD; $n = 5$) with asterisks represent significant differences between treatments (Student test; $P < 0.05$).

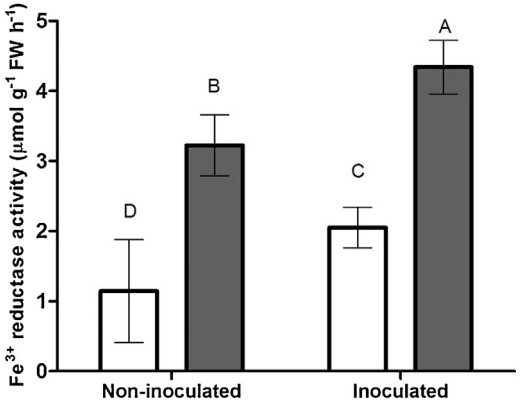

Fig. 6. FRO activity in roots of plants grown in an alkaline environment. FRO activity was determined after 15 d. White bars represent control treatments and grey bars represent alkaline treatments (mean ± SD; $n = 5$). Different letters indicate significant differences among treatments. Duncan test, two-way ANOVA ($P < 0.05$).

level of 7.98 RU with respect to the non-inoculated controls; this effect was correspondingly amplified for the stressed inoculated samples, which showed a level of 20.25 RU versus the inoculated controls (Fig. 7a). However, analysis of the *IRT1* gene showed no regulation under alkaline conditions for the non-inoculated plants. In contrast, inoculation induced an increase in expression, giving a mean value of 5.5 RU for the stress treatment and 0.92 RU for the control (Fig. 7b).

4. Discussion

Ahmed and Holmström (2014) reported that the primary function of siderophores is to chelate Fe^{3+} from different terrestrial habitats, thereby making it available to microbial and plant cells. The mechanisms involved in plant Fe-uptake mediated by microbial siderophores are as yet unclear; however, there is abundant evidence showing that the soil microorganisms that produce siderophores play an important role in favoring Fe assimilation in constrained environments (Sharma and Johri, 2003; Crowley et al., 1988; Jin et al., 2010; Vansuyt et al., 2007; Nagata et al., 2013). In our studies, the Fe^{2+} content in the shoots of Gifu plants cultivated under alkaline conditions was lower than in plants cultivated under control conditions. This is consistent with our recent research (Babuin et al., 2014), suggesting the sensitive nature of this ecotype to alkaline stress. These results, together with the chlorosis phenotype observed in plants grown under alkaline conditions, reveal a flaw in Fe^{2+} translocation from the roots to the shoots. This is also consistent with the observed reduction in PSII performance (Babuin et al., 2014). However, inoculation improved the nutrient balance for those plants, resulting in high endogenous Fe^{2+} content in the shoots, with accompanying greening in young leaves and recovery of PSII performance. Likewise, these plants retained their relative DW, attaining values similar to those of the non-inoculated control plants and confirming the plant growth-promoting effect of *P. eucalypti* M91.

The increase in Fe^{2+} content in the shoots of the inoculated plants can be attributed to an increase in the gene expression of Fe^{3+} reductases and transporters responsible for the incorporation of Fe^{2+} through Strategy I. Particularly, *FRO1* gene expression correlates with an increase in the activity of the FRO1 reductase enzyme. This may be explained by an increase in the amount of Fe^{3+} bio-availability in the rhizosphere, chelated as Fe^{3+}-siderophores. Given that the production of these compounds is higher under alkaline conditions, a greater concentration of Fe^{3+} would be available to act as a substrate for the Fe^{3+} reductase. Likewise, an increase in *FRO1* and *IRT1* expression levels was also seen with *Bacillus subtilis* inoculation of *Arabidopsis* (Zhang et al., 2009), in which case the bacterial production of volatile organic compounds (VOCs) triggered an increase in *FRO2* and *IRT1* expression. VOC and organic acid

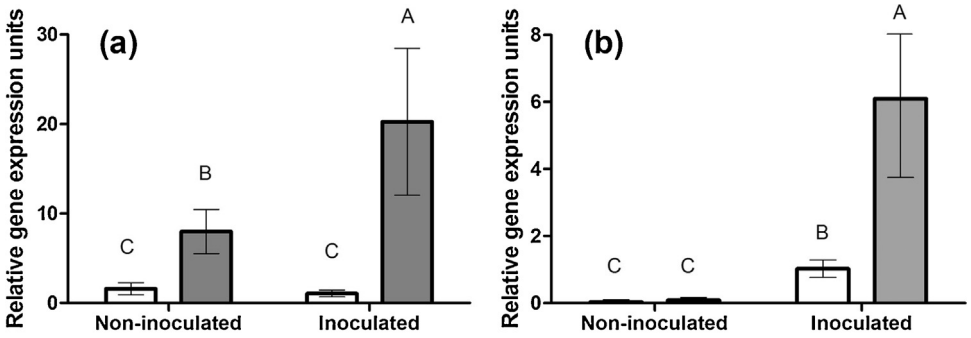

Fig. 7. Regulation of plant genes involved in the assimilation of soil Fe. (a) *FRO1* and (b) *IRT1* gene expression in Gifu plants after 21 days of alkaline treatment. White bars represent control treatment and grey bars represent alkaline treatment (mean ± SD; $n = 3$). Different letters indicate significant differences among treatments. Duncan test, two-way ANOVA ($P < 0.05$).

production has also been measured in other species of the genus *Pantoea* (Cimmino et al., 2006; Dastager et al., 2009).

It has been reported that phosphate solubilization mediated by *Pantoea* and other species is mainly due to acidification of the medium by these produced VOCs and organic acids (Dastager et al., 2009). Our laboratory previously reported that *P. eucalypti* M91 can solubilize phosphates mainly by inducing the secretion and subsequent oxidation of gluconic acid (Castagno et al., 2011). For this reason, we set out to determine the effect of inoculation on solution acidification. The observed acidification under both control and alkaline conditions could also be partly responsible for increasing Fe solubility and converting it into a form more available to the plant through transporter proteins like IRT1. This could explain why increased expression of *IRT1* was observed in both the alkaline and control trials of the inoculated plants, but not in the non-inoculated trials, which, again, is consistent with results obtained by both Babuin et al. (2014) and Zhang et al. (2009).

Similarly, it has previously been reported that root architecture is affected by many soil properties, including mechanical strength and density, soil pH and temperature, and a variety of nutrient deficiencies and biotic interactions (Smith and De Smet, 2012). The efficient use of Fe by plants has been related to their capacity to develop not only specific physiological responses, but also morphological responses in the root when Fe is limited. In earlier studies, we found that certain *L. japonicus* ecotypes can efficiently use Fe when exposed to alkaline conditions by modifying their root morphology, while others that fail to do so are less efficient (unpublished data). Further results suggest that root topology could be an important factor more generally with respect to alkaline tolerance in the genus *Lotus* (Paz et al., 2012). While non-inoculated plants in this study did not modify their root morphology from a dichotomous pattern when exposed to alkaline stress, those that were inoculated took on a herringbone topology.

Many previous works have shown that PGPB strains can cause alterations in the root architecture of host plants by promoting the formation of secondary roots, thus improving exploratory capacity (Marschner et al., 2011; Zamioudis et al., 2013). Lateral root initiation is the result of auxin-dependent cell cycle progression in a specific subset of the pericycle cells (Smith and De Smet, 2012). As such, the formation of a great number of lateral roots in the inoculated plants could be due to bacterial auxin production, considering that rhizospheric microorganisms can promote plant growth by improving nutrient assimilation or by phytohormone production (Hayat et al., 2010; Jin et al., 2014). Although our studies have not detected indole-3-acetic acid (IAA) in the growth medium, we cannot rule out the possibility that *P. eucalypti* M91 may produce phytohormones under the plant growth conditions evaluated. This possibility is supported by a paper by Dastager et al. (2009), who isolated and characterized a strain of *Pantoea* spp. and found IAA production. Moreover, Cimmino et al. (2006) also found IAA production in several strains of *P. agglomerans*.

In addition, the role of 14-3-3 proteins in cell elongation has recently been addressed. Some of the suggested mechanisms include the regulation of hormone signaling pathways and alterations in the activity of H^+-ATPases (Xu and Shi, 2006; Denison et al., 2011; Xu et al., 2012). Interestingly, the interaction of these proteins with other target proteins can also be altered by increasing external stimuli to up-regulate defense responses within the plant. This stimulus may somehow come from inoculation with *P. eucalypti* M91.

Taking all of this into account, it can be seen that *P. eucalypti* M91 not only promotes morphological and biochemical changes, but also molecular responses, triggering the activation of the "plant machinery" to optimize Fe metabolism and, as a result, improve the photosynthetic performance of this Fe-inefficient plant species. Moreover, in addition to its recognized ability to solubilize phosphorus, its ability to increase plant-available levels of Fe should be highlighted. These features make *P. eucalypti* M91 a potential tool for improving the performance of economically important crops in nutritionally-deficient soils. Furthermore, it could be used with members of the *Lotus* genus in soil reclamation and the restoration of degraded pastures.

5. Conclusion

Inoculating the Fe-inefficient Gifu ecotype of *L. japonicus* with the endophytic PGPB *P. eucalypti* M91 was shown to induce physiological and morphological changes consistent with Strategy I plants, thereby improving the resistance to alkaline stress of this normally sensitive ecotype. This occurs through improved Fe translocation and photosynthetic performance.

Acknowledgments

The authors wish to thank Patricia Uchiya of the Comisión de Investigaciones Científicas de la Provincia de Buenos Aires (CIC, Argentina) for her valuable assistance and Dr. Guillermo Santamaría for his generous support in assessing total iron determination. This study was supported by the Consejo Nacional de Investigaciones Científicas y Técnicas (CONICET, Argentina), Agencia Nacional de Promoción Científica y Tecnológica through the Proyectos de Investigación Científica y Tecnológica (PICT, Argentina), CIC, and Universidad Nacional de San Martín (Argentina). MPC is a postdoctoral fellow of CONICET, MJE is a research member of the CIC, and LNC and OAR are researchers for CONICET.

Appendix A. Supplementary data

Supplementary data associated with this article can be found, in the online version, at http://dx.doi.org/10.1016/j.jplph.2016.01.001.

References

Abadia, J., Morales, F., Abadia, A., 2000. Photosystem II efficiency in low chlorophyll, iron-deficient leaves. Plant Soil 215, 183–192.

Ahmed, E., Holmström, S.J., 2014. Siderophores in environmental research: roles and applications. Microb. Biotechnol. 7, 196–208.

Babuin, M.F., Campestre, M.P., Rocco, R., Bordenave, C.D., Escaray, F.J., Antonelli, C., et al., 2014. Response to long-term $NaHCO_3$-derived alkalinity in model *Lotus japonicus* ecotypes Gifu B-129 and Miyakojima MG-20: transcriptomic profiling and physiological characterization. PLoS One, http://dx.doi.org/10.1371/journal.pone.0097106.

Bacaicoa, E., García-Mina, J.M., 2009. Iron efficiency in different cucumber cultivars: the importance of optimizing the use of foliar iron. J. Am. Soc. Hortic. Sci. 134, 405–416.

Carrillo, G.C., Peralta, J.R.V., 1988. Siderophore-like activities in *Rhizobium phaseoli*. J. Plant Nutr. 11, 935–944.

Bordenave, C.D., Escaray, F.J., Menendez, A.B., Serna, E., Carrasco, P., Ruiz, O.A., Gárriz, A., 2013. Defense responses in two ecotypes of *Lotus japonicus* against non-pathogenic *Pseudomonas syringae*. PLoS One 8, e83199.

Castagno, L.N., Estrella, M.J., Sannazzaro, A.I., Grassano, A.E., Ruiz, O.A., 2011. Phosphate-solubilization mechanism and in vitro plant growth promotion activity mediated by *Pantoea eucalypti* isolated from *Lotus tenuis* rhizosphere in the Salado River Basin (Argentina). J. Appl. Microbiol. 110, 1151–1165.

Castagno, L.N., García, I.V., Sannazzaro, A.I., Bailleres, M., Ruiz, O.A., Mendoza, R.E., Estrella, M.J., 2014. Growth, nutrient uptake and symbiosis with rhizobia and arbuscular mycorrhizal fungi in *Lotus tenuis* plants fertilized with different phosphate sources and inoculated with the phosphate-solubilizing bacterium *Pantoea eucalypti* M91. Plant Soil 385, 357–371.

Cimmino, A., Andolfi, A., Marchi, G., Surico, G., Evidente, A., 2006. Phytohormone production by strains of *Pantoea agglomerans* from knots on olive plants caused by *Pseudomonas savastanoi* pv. *savastanoi*. Phytopathol. Mediterr. 45, 247–252.

Crowley, D.E., Reid, C.P.P., Szaniszlo, P.J., 1988. Utilization of microbial siderophores in iron acquisition by oat. Plant Physiol. 87, 680–685.

Dastager, S.G., Deepa, C.K., Puneet, S.C., Nautiyal, C.S., Pandey, A., 2009. Isolation and characterization of plant growth-promoting strain *Pantoea* NII-186 from Western Ghat forest soil, India. Lett. Appl. Microbiol. 49, 20–25.

Denison, F.C., Paul, A.-L., Zupanska, A.K., Ferl, R.J., 2011. 14-3-3 proteins in plant physiology. Semin. Cell Dev. Biol. 22, 720–727.

Dumas, Z., Ross-Gillespie, A., Kümmerli, R., 2013. Switching between apparently redundant iron- uptake mechanisms benefits bacteria in changeable environments. Proc. Biol. Sci. 280, 1764.
Eichert, T., Peguero-Pina, J.J., Gil-Pelegrín, E., Heredia, A., Fernández, V., 2010. Effects of iron chlorosis and iron resupply on leaf xylem architecture, water relations, gas exchange and stomatal performance of field-grown peach (*Prunus persica*). Physiol. Plant 138, 48–59.
Escaray, F.J., Menendez, A.B., Gárriz, A., Pieckenstain, F.L., Estrella, M.J., Castagno, L.N., et al., 2012. Ecological and agronomic importance of the plant genus *Lotus:* its application in grassland sustainability and the amelioration of constrained and contaminated soils. Plant Sci. 182, 121–133.
Gazquez, A., Maiale, S.J., Rachoski, M.M., Vidal, A., Ruiz, O.A., Menéndez, A.B., Rodríguez, A.A., 2015. Physiological response of multiple contrasting rice (*Oryza sativa* L.) cultivars to suboptimal temperaturas. J. Agric. Crop Sci. 201, 117–127.
Guerinot, M.L., Yi, Y., 1994. Iron: nutritious, noxious, and not readily available. Plant Physiol. 104, 815–820.
Hayat, R., Safdar Ali, S., Amara, U., Khalid, R., Ahmed, I., 2010. Soil beneficial bacteria and their role in plant growth promotion: a review. Ann. Microbiol. 60, 579–598.
Hoagland, D.R., Arnon, D.I., 1950. The water-culture method for growing plants without soil. Calif. Agric. Exp. Stn. 347, 32.
Ivanov, R., Brumbarova, T., Bauer, P., 2012. Fitting into the harsh reality: regulation of iron-deficiency responses in dicotyledonous plants. Mol. Plant 5, 27–42.
Jain, A., Wilson, G.T., Connolly, E.L., 2014. The diverse roles of FRO family metalloreductases in iron and copper homeostasis. Front. Plant Sci. 5, 100.
Jin, C.W., Li, G.X., Yu, X.H., Zheng, S.J., 2010. Plant Fe status affects the composition of siderophore-secreting microbes in the rhizosphere. Ann. Bot. 105, 835–841.
Jin, C.W., Ye, Y.Q., Zheng, S.J., 2014. An underground tale: contribution of microbial activity to plant iron acquisition via ecological processes. Ann. Bot. 113, 7–18.
Klein, M., López-Millán, A.F., Grusak, M.A., 2012. Quantitative trait locus analysis of root ferric reductase activity and leaf chlorosis in the model legume *Lotus japonicus*. Plant Soil 351, 363–376.
Koch, B., Jensen, L.E., Nybroe, O., 2001. A panel of *Tn7*-based vectors for insertion of the gfp marker gene or for delivery of cloned DNA into Gram-negative bacteria at a neutral chromosomal site. J. Microbiol. Methods 45, 187–195.
Larbi, A., Abadia, A., Abadia, J., Morales, F., 2006. Down co-regulation of light absorption, photochemistry, and carboxylation in Fe-deficient plants growing in different environments. Photosynth. Res. 89, 113–126.
Marschner, P., Crowley, D., Rengel, Z., 2011. Rhizosphere interaction between microorganisms and plants govern iron and phosphorus acquisition along the root axis model and research methods. Soil Biol. Biochem. 43, 883–894.
Nagata, T., Oobo, T., Aozasa, O., 2013. Efficacy of a bacterial siderophore, pyoverdine, to supply iron to *Solanum lycopersicum* plants. J. Biosci. Bioeng. 115, 686–690.
Paz, R.C., Rocco, R.A., Reinoso, H., Menéndez, A.B., Pieckenstain, F.L., Ruiz, O.A., 2012. Comparative study of alkaline, saline, and mixed saline—alkaline stresses with regard to their effects on growth, nutrient accumulation, and root morphology of *Lotus tenuis*. J. Plant Growth Regul. 31, 448–459.
Radzki, W., Gutiérrez Mañero, F.J., Algar, E., Lucas García, J.A., Garcia-Villaraco, A., Ramos Solano, B., 2013. Bacterial siderophores efficiently provide iron to iron-starved tomato plants in hydroponics culture. Antonie Van Leeuwenhoek 104, 321–330.
Ramírez, L., Graziano, M., Lamattina, L., 2008. Decoding plants adaptive responses to iron deficiency: Is nitric oxide a central player? Plant Signal. Behav. 3, 795–797.
Romera, F.J., Garcia, M.J., Alcantara, E., Perez-Vicente, R., 2011. Latest findings about the interplay of auxin, ethylene and nitric oxide in the regulation of Fe deficiency responses by Strategy I plants. Plant Signal. Behav. 6, 167–170.
Sanchez, D.H., Pieckenstain, F.L., Escaray, F., Erban, A., Kraemer, U., Udvardi, M.K., Kopka, J., 2011. Comparative ionomics and metabolomics in extremophile and glycophytic Lotus species under salt stress challenge the metabolic pre-adaptation hypothesis. Plant Cell Environ. 34 (4), 605–617.
Schwyn, B., Neilands, J.B., 1987. Universal chemical assay for the detection and determination of siderophores. Anal. Biochem. 160, 47–56.
Sharma, A., Johri, B.N., 2003. Combat of iron-deprivation through a plant growth promoting fluorescent *Pseudomonas* strain GRP3A in mung bean (*Vigna radiate* L. Wilzeck). Microbiol. Res. 158, 77–81.
Singh, S.P., Vogel-Mikuš, K., Arčon, I., Vavpetič, P., Jeromel, L., Pelicon, P., Kumar, J., Tuli, R., 2013. Pattern of iron distribution in maternal and filial tissues in wheat grains with contrasting levels of iron. J. Exp. Bot. 64, 3249–3260.
Smith, S., De Smet, I., 2012. Root system architecture: insights from *Arabidopsis* and cereal crops. Philos. Trans. R Soc B 367, 1441–1452.
Sperry, J.F., Wilkins, T.D., 1976. Arginine, a growth-limiting factor for Eubacterium lentum. J. Bacteriol. 127, 780–784.
Strasser, R.J., Srivastava, A., Tsimilli-Michael, M., 2000. The fluorescence transient as a tool to characterize and screen photosynthetic samples. In: Yunus, M., Pathre, U., Mohanty, P. (Eds.), Probing Photosynthesis: Mechanisms, Regulation and Adaptation. Taylor and Francis, London, pp. 445–483.
Vansuyt, G., Robin, A., Briat, J.F., Curie, C., Lemanceau, P., 2007. Iron acquisition from Fe-pyoverdine by *Arabidopsis thaliana*. Mol. Plant Microbe Interact. 20, 441–447.
Von Wirén, N., Romheld, V., Marschner, H., 1993. Evaluation of strategy I mechanisms in iron efficient and inefficient maize cultivars. Plant Soil 155/156, 445–448.
Wang, B., Li, Y., Zhang, W.H., 2012. Brassinosteroids are involved in response of cucumber (*Cucumis sativus*) to iron deficiency. Ann. Bot. 110, 681–688.
Xiao, R., Kisaalita, W.S., 1995. Purification of pyoverdines of pseudomonas fluorescens 2-79 by copper-chelate chromatography. Appl. Environ. Microbiol. 61, 3769–3774.
Xu, W.F., Shi, W.M., 2006. Expression profiling of the 14-3-3 gene family in response to salt stress and potassium and iron deficiencies in young tomato (*Solanum lycopersicum*) roots: analysis by real-time RT–PCR. Ann. Bot. 98, 965–974.
Xu, W., Jia, L., Shi, W., Liang, J., Zhang, J., 2012. Smart role of plant 14-3-3 proteins in response to phosphate deficiency. Plant Signal. Behav. 7, 1047–1048.
Yang, B., Hoegy, F., Mislin, G.L.A., Mesini, P.J., Terbium, Schalk I.J., 2011. a fluorescent probe for investigation of siderophore pyochelin interactions with its outer membrane transporter FptA. J. Inorg. Biochem. 105, 1293–1298.
Zamioudis, C., Mastranesti, P., Dhonukshe, P., Blilou, I., Pieterse, C.M., 2013. Unraveling root developmental programs initiated by beneficial *Pseudomonas* spp. bacteria. Plant Physiol. 162, 304–318.
Zhang, H., Sun, Y., Xie, X., Kim, M.S., Dowd, S.E., Paré, P.W., 2009. A soil bacterium regulates plant acquisition of iron via deficiency-inducible mechanisms. Plant J. 58, 568–577.
Zouari, M., Abadia, A., Abadia, J., 2001. Iron is required for the induction of root ferric chelate reductase activity in iron-deficient tomato. J. Plant Nutr. 24, 383–396.